TRIUMF Experiment E614
Technical Note #71

Energy Resolution Optimization of the Target PCs and $t_\circ$ Problem

V.I. Selivanov
24 September 2002

1 Wire chambers in proportional mode.
Review of experimental data

Measurement of a particle energy by a wire chamber requests a linear dependence (proportional mode) of ADC channel number (accumulated charge) from the particle deposit energy in the chamber. An example of the mode presented in Fig.1 [1]. The expected exponential dependence of the gain from high voltage for the proportional mode demonstrates in Fig.2 [2] lower than $2.6 - 2.8kV$. A saturated mode appears at $HV > 2.8keV$. That been explained by an electric field screening near wire by an positive ion cloud of an avalanche. Therefore a minimal value of the saturating HV depends from number of primary electrons produced by a particle. For example, one can have a proportional mode for a relativistic particle with electron number of $\simeq$ 50e per 4mm, but a saturated mode for ^{55}Fe source with $\simeq$ 200e. One can see from Fig.3 [3] that energy resolution worsening from 18% in proportional mode at HV=2.0 kV to 50% in saturated mode at HV=3.0kV. Fig.4 [4] demonstrates a proportional mode till gain more than 10^5 for $Ar/C_2H_6(50/50)$, $Ar/ISO(70/30)$ and $Ar/ISO(29/71)$ drift gases. Drift gases with CF_4 have not so wide range of a proportional mode as that demonstrated in Fig.5 [4]. Authors of the article explained this fact by a high electron attachment for CF_4 in avalanche area. It has been confirmed by Garfield calculations (See next Section).

Dependence of energy resolution from a deposit energy in chamber for $E_\gamma = 6 - 30keV$ is presented in Fig.1. The dependence can be described as $\sigma(E)/E \sim 1/\sqrt{dE}$ and can be extrapolated to $E_\gamma > 30keV$. Results of the estimation are presented in Table 1.
The energy resolution values are presented as circles with radius of σE in Fig.6 taken from [5]. One

Table 1: Total number of electrons in PC end energy resolution for sources with several particle energy. $^{(*)}$ - measured in [1] ,$^{(**)}$ - estimation.

Source	e^+, $50MeV/c$	Fe^{55}, γ $5.9keV$	Am^{241}, γ $30keV$	dE, μ^+ $100keV$	dE, μ^+ $200keV$	dE, μ^+ $300keV$
Total number of electrons	60	200	1,030	3,400	6,800	13,400
Resolution, $\sigma E(keV)$	–	$0.51^{(*)}$	$1.3^{(*)}$	$2.3^{(**)}$	$3.2^{(**)}$	$4.1^{(**)}$

can see that even two times worse energy resolution will provide a good selection of muons stopped in PC6. However we have not any selection of the muons stopped in PC6 according [6]. It seems we have several explanations of that.

1.Using of a gas with a bad energy resolution, for example, a gas with CF_4 admixture.
or/and

2.Using a gas in saturation mode.
or/and
3.Saturation of VTX.
or/and
4.Not so good dividing of a wire signal between TDC and ADC VTXs.

The possible reasons are analyzed below.

2 GARFIELD calculations

GARFIELD calculations have been done for $CF_4/ISO(80 : 20)$, $Ar/ISO(40 : 60)$, and $Ar/CH_4(90 : 10)$ gases. The last one has gain till 10^8, but it been excluded from analysis because a big Lorentz close to 90° at B=2T (see Fig.24). GARFIELD program calculates a gain with a big error and does not calculate saturation effects. Therefore the calculations have not been done. Existing PC cell with sense wire diameter of $15\mu m$, anode cathode gap of 1.997mm, and wire spacing of 2mm been used. Figs.1-24, 26 demonstrate some drift parameters for the gases. Comparison of Fig.9 and 10 shows the attachment coefficient for CF_4/ISO gas in $\simeq$ 100 times larger then for Ar/ISO gas. Therefore using of the CF_4/ISO gas for target PCs is questionable, but one can not exclude this possibility at a low HV value because $CF_4/ISO(50 : 50)$ gas has linearity till gain of $4 \cdot 10^3$ according to Fig.5. The using is possible if we have sufficient sensitivity of our ADC. Far better proportional range till 10^6 has Ar/ISO gases according to Fig.4. $Ar/ISO(40 : 60)$ gas has less drift velocity than $CF_4/ISO(80 : 20)$ according to Figs.7, 8, but less Lorentz drift angle at B=2T according to Figs.11, 12. Therefore several types of drift times have been calculated. Drift time of ALL electrons from a particle track going exactly between nearest cells equals to infinity if a particle has not a scattering. But a low energy muon has a remarkable scattering as that demonstrate Figs.15, 16. One can see secondary delta electron tracks also. Figs.15, 16 are calculated at $E_{\mu^+} > 2.5MeV$ because GARFIELD package has a limited number of electrons for a drift lines representation. Rest figures have been calculate at $E_{\mu^+} = 1.0MeV$. This energy corresponds to muons stopping in downstream wall of a $20mg/cm^2$ target. One can see from Figs.18, 20 that a full time collection of ALL electrons from a muon track going at X=1mm exactly between nearest cells is less than $0.3\mu s$. In reality muon losses from 30 to 300 keV according to Fig.6. Therefore we can neglect of LAST 100 electrons because it corresponds to an insignificant energy shift of 0.13 keV at dE=30 keV and 0.03 keV at dE=300 keV according to Table 1. Fig.23 presents a maximum drift time dependence of LAST-50 and LAST-150 electron vs HV. We can conclude from the Fig.23 that a necessary gate width for ADC is $\simeq 200ns$ even at HV=800V for both gases.

3 Wire output circuit

Fig.25 presents the circuit in rough outline. Value of $C_2 \simeq 1000pF$ and $R_2 \simeq 1000\Omega$ are used now. Therefore we have two parallel-connected circuits with different time constants τ for a current pulse from a wire: $\tau_{TDC} = 15.6ns$ and $\tau_{ADC} \simeq 120ns$. It means different dividing coefficient between the circuits as function of pulse width from wire. For example, the dividing coefficient is $\simeq 1/10$ for the ADC circuit at pulse width of $T << 15ns$ and it is much more at $T >> 15ns$. $\tau_{TDC} = \tau_{ADC}$ is optimal value for a constant dividing at any pulse width value. It corresponds to $C_2 \simeq 15pF$ at $R_2 = 1000\Omega$.

4 $t_\circ$ problem

Using of TDC and ADC circuits together on an one wire output is a questionable problem because a gas saturation requests a low gain value for a correct measurement of accumulated charge. According an estimation we have now gain $\simeq 5{\cdot}10^3$ from PCs at HV=1950V. It corresponds to $\simeq 3{\cdot}10^5 e(1.9{\cdot}10^{-2}pC)$ collected charge for a relativistic particle and $\simeq 6.7\cdot 10^7 e(4.4pC)$ for deposit muon energy of 300keV. One can see from Fig.2 that $4.4{\cdot}10^{-2}pC$ corresponds to the proportional mode, and 4.4pC corresponds to a deep saturated mode. We have to decrease PC gain to have a proportional mode for good ADC resolution and will loss, of course, the chambers sensitivity for decaying positrons and will loss also $t_\circ$ for DCs. Therefore one needs to estimate two possibilities for $t_\circ$.

4.1 $t_\circ$ from target PCs

∗ It is done and it works.
∗ One can estimate a dead zone size in U-wire of PC6 after muon track arrival. The dead zone corresponds to angle in V-direction of $\theta_V \simeq 50°$ if muon hits two nearest wires, and to angle $\theta_V \simeq 15°$ if muon hits one wire. Muon has a remarkable probability to hit both nearest wires because a big scattering (see Fig.26). We should use $\theta_V \simeq 40°$ for further estimations. A dead zone along wire in U-direction can have length to 0.5mm because a big scattering (Fig.26). It corresponds to angle of $\theta_U \simeq 15°$. This dead zone can be shifted on 1mm because Lorentz drift angle (see Fig.13). The shift depends on a distance X between wire and track. The maximum shift of 1mm corresponds to angle $\theta_{U_{shift}} \simeq 45°$. So, we have a complicated picture for U-direction. Let me suggest that we will have a dead zone inside a cone with polar angle $\theta = 45°$ around upstream direction. Time resolution inside the zone is defined by PC5 only. The resolution will be $\simeq 6ns$ (RMS) according to Fig.27. Time resolution outside the cone is defined by both PC5 and PC6. The resolution is $\simeq 2ns$ (Fig.27) [7]. One can estimate what we will have if to reject from a further analysis the cone using the "FIRST GUESS" package. All Michel parameters have a low sensitivity inside the cone (see Figs.E.1-E.4 in [8]). It seems we will loss a small part of a statistical precision excluding the cone. That needs to be confirm with Monte Carlo simulations. Let me remark that all Michel parameters can be measured with 10^{-3} accuracy only excluding the cone because we will have a low precision of energy calibration for the upstream part of the detector.
∗ Measurement of $P_\mu\xi$ parameter requests a good ADC analysis from PC5 and PC6 to select muons stopped in PC6 gas. Measurement of rest Michel parameters with accuracy of $\simeq 10^{-4}$ requests a good $t_\circ$ definition in area of $\theta = 10° - 60°$. All that excludes using of the target PCs as $t_\circ$ master for positron registration. Therefore one has estimate a possibility of using PC1-PC4 as $t_\circ$ master.

4.2 $t_\circ$ from PC1-PC4

∗ One can estimate a dead zone size in a U-wire of PC1-PC4 after muon track arrival. Muon on entrance of the PCs has energy $E_{\mu^+} \simeq 2.5MeV$. Its scattering does not exceed 0.1mm as one see from Fig.16. It means the muon will hit two nearest cells with a low probability because the beam has divergence $\theta < 50mrad$. A dead zone in V-direction with length of 2.2mm instead of 4.0mm for $E_{\mu^+} < 1.0MeV$ will be used for further estimations. An avalanche length along the wire is about 0.2mm according to Fig.13. Therefore the dead zone square is $S_d = 2.2 \times 0.2mm^2$. Probability to hit the zone by an outgoing positron is $R_d = S_d/S_{E_e}$, where S_{E_e} is square covered by a positron helix with energy E and polar angle of θ. The ratio is $R_d \simeq 5\cdot 10^{-6}$ for $E_\mu = 50MeV$ and $\theta = 90°$, and $R_d \simeq 2\cdot 10^{-5}$ for $E_\mu = 50MeV$ and $\theta = 30°$. Estimations have been done for an isotropic in angle distribution. Statistical spread for 10^9 events is $3\cdot 10^{-5}$. It means one can measure $1/cos\theta$ dependence with range of $\theta = 30° - 60°$, and can reach an adequate accuracy of positron energy determination. R_d value is less of course at $E_e < 50MeV$, but one can exclude the events from further analysis because a

low sensitivity of Michel parameters to the energy. Probability to hit a cross-section between U and V dead zones is very small. It is $1.1 \cdot 10^{-5}$ for muon with $E_\mu = 20MeV$ and $\theta = 30°$. Sequence PC1 - U and PC2 - V will provide $t_\circ$ without a remarkable loss of events. Time resolution (RMS) will be $\simeq 2ns$ if muon does not hit a dead zone, and $\simeq 6ns$ if muon hits a dead zone [7]. And more, muon losses in first PCs about 12keV/plane according to Fig.10 in [9] compare with (30-300)keV/PC6 (Fig.6). It means a smaller influence of a muon track on outgoing positron registration.
$*$ The proposed upgrade requests some job and some number of VTX. It seems we have enough number of VTXs for the upgrade.
$*$ Question about the possibility to use PC1 and PC2 chamber for $t_\circ$ definition requests a Monte Carlo simulation to determine a real R_d value. Insertion of a same gap between the PC planes decreases the R_d value. Best solution, probably, is a sequence $(U_1 + V + U_2)$ with a gap of 40mm between them. U_2-plane can have, for example, 48 sense wires in central area.

References

[1] I. Lehraus, R. Matthewson, W. Tejessy, M. Aderholz, Performance of a large Scale Multilayer Ionization Detector and its use for Measurements of the relativistic Rise in the Momentum Range of $20 - 110GeV/c$, Nucl. Instr. Meth. 153(1978)347-355 .

[2] A.I. Mincer, S. Dado, J.J. Goldberg, Y. Gernitzky, D. Lasic, N.Z. Lupu, S. Robins, Y. Rosen, S. Tarem, Charge Production in thin Gap multi-wire Chambers, Nucl. Instr. Meth. A439(2000)147-157 .

[3] H. Okuno, N. Khalatyan, Y. Nakamura, K. Fujii, K. Hoshina, Y. Kato, Y. Kurihara, O. Nitoh, Gas Gain Study for $CO_2/isobutane$ Mixture, Nucl. Instr. Meth. A447(2000)459-466 .

[4] W.S. Anderson, J.C. Armitage, E. Dunn, J.G. Heinrich, C. Lu, K.T. McDonald, J. Weckel, Y.Zhu, Electron Attachment, effective ionization Coefficient, and Electron Drift Velocity for CF_4 Gas Mixtures, Nucl. Instr. Meth. A323(1992)273-279 .

[5] M. Grinder and D.H. Wright, An Analysis of Energy Loss in the Proportional Chambers near the Target, TN-22, 1998 .

[6] M. Lalancette, Report on Energy Loss Analysis in the Proportional Chambers near the Target, TN-70, 2002 .

[7] Y.Y. Lachin, L.V. Miassoedov, I.V. Morozov, V.I. Selivanov, I.V. Sinitzin, V.D. Torokhov, Wire chamber as a fast, high efficiency and low mass trigger in high magnetic fields, Nucl. Instr. Meth. A361(1995)77-84, and TN-20, 1998 .

[8] Precise measurement of the ρ, δ and $P_\mu\xi$ Parameters in Muon Decay, Original E614 Proposal, Jule 12 1990 .

[9] D.H. Wright, Monte Carlo Summary Report to the E614 Collaboration, TN-21, 1998 .

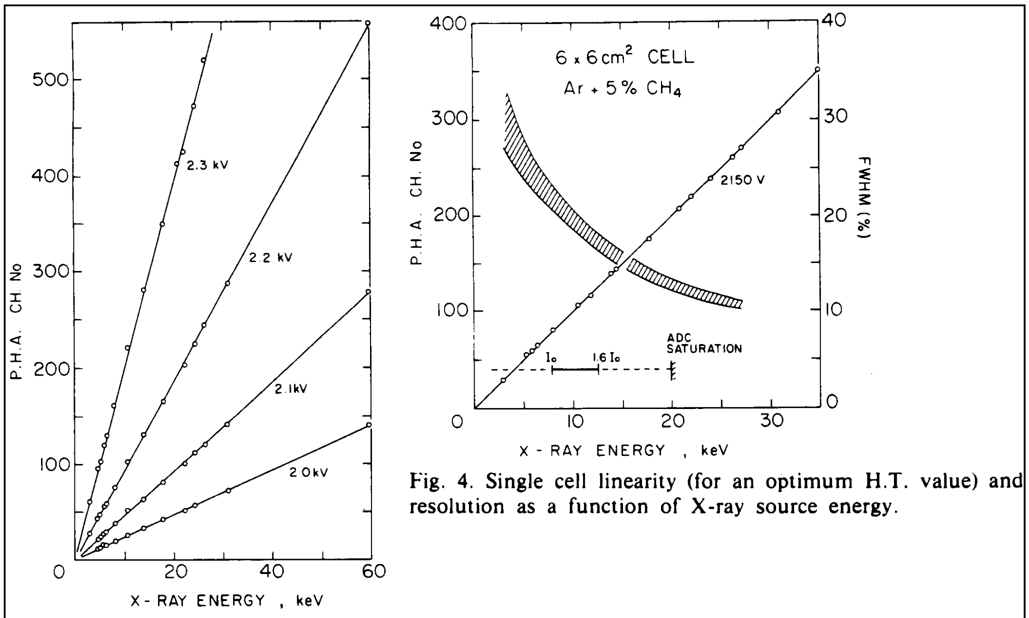

Fig. 3. Linearity of a single cell response to X-ray energy deposit for several H.T. settings.

Fig. 4. Single cell linearity (for an optimum H.T. value) and resolution as a function of X-ray source energy.

Figure 1: Single cell linearity and resolution as a function of X-ray source energy [1].

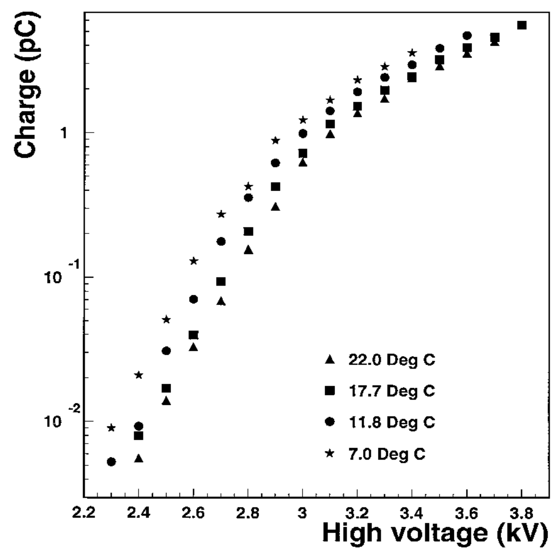

Fig. 12. Measured charge as a function of high voltage applied to a chamber with wire spacing 0.18 cm and anode cathode gap of 0.14 cm for gas mixed at various temperatures.

Figure 2: Measured charge as a function of high voltage with different fraction on n-pentane [2]. Wire spacing 1.8mm, anode cathode gap 1.4mm, gas $n - pentane/CO_2$. ^{106}Ru with maximum electron energy of $3.54MeV$ has been used.

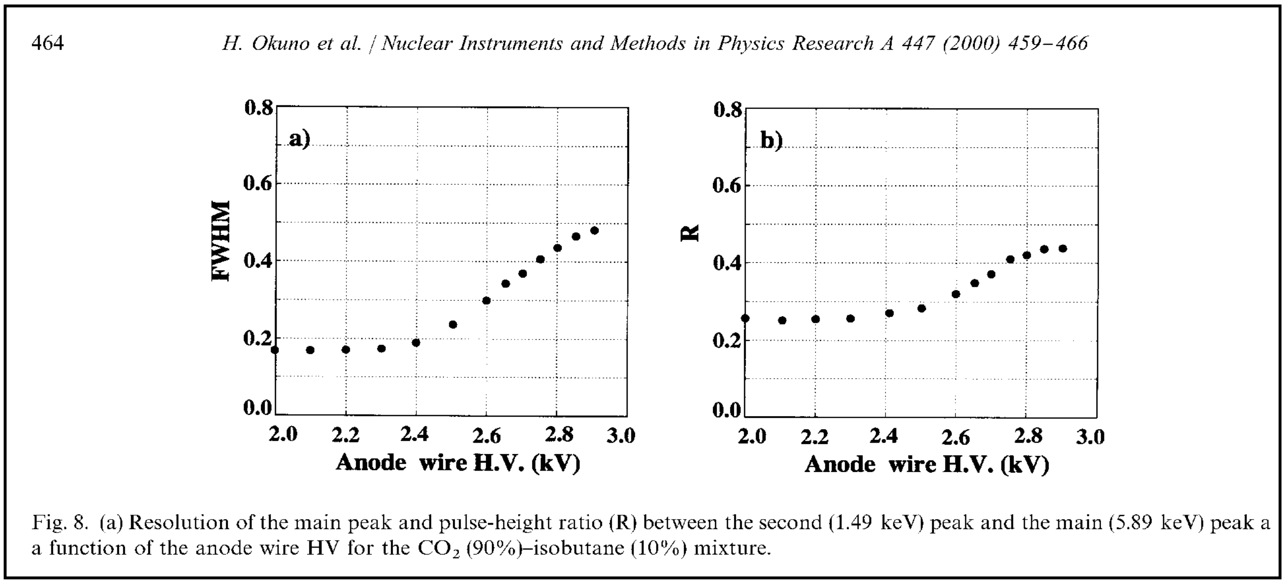

Figure 3: Demonstration of transition from proportional to saturated mode at $HV \simeq 2.4kV$ [3].

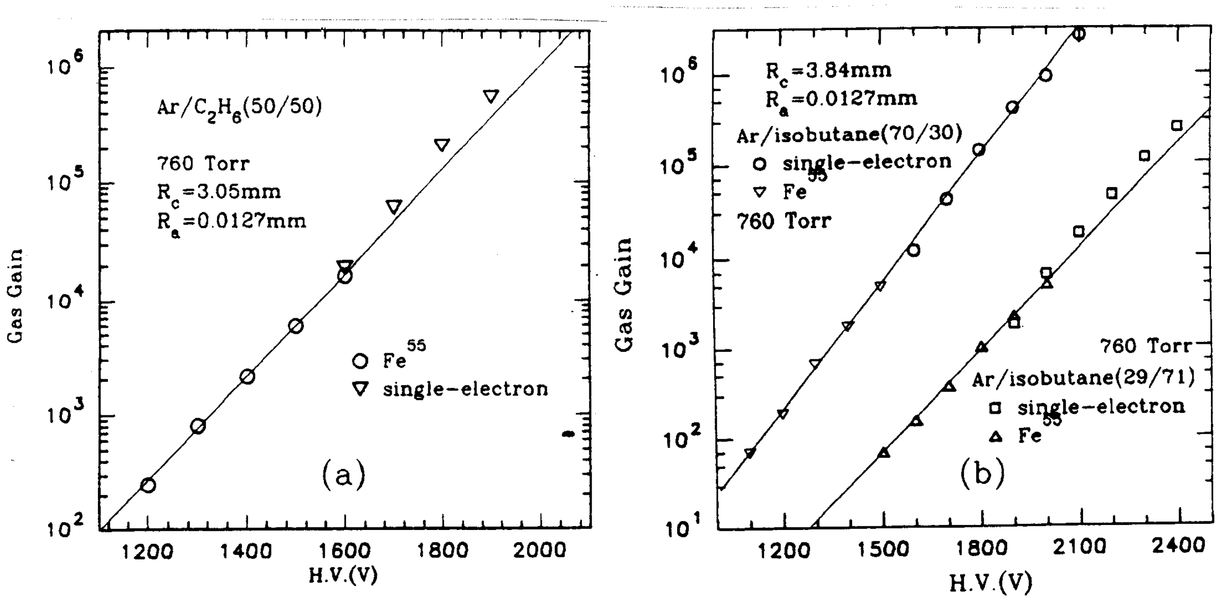

Figure 4: Exponential growth of gain till $> 10^5$ for several gas mixtures [4].

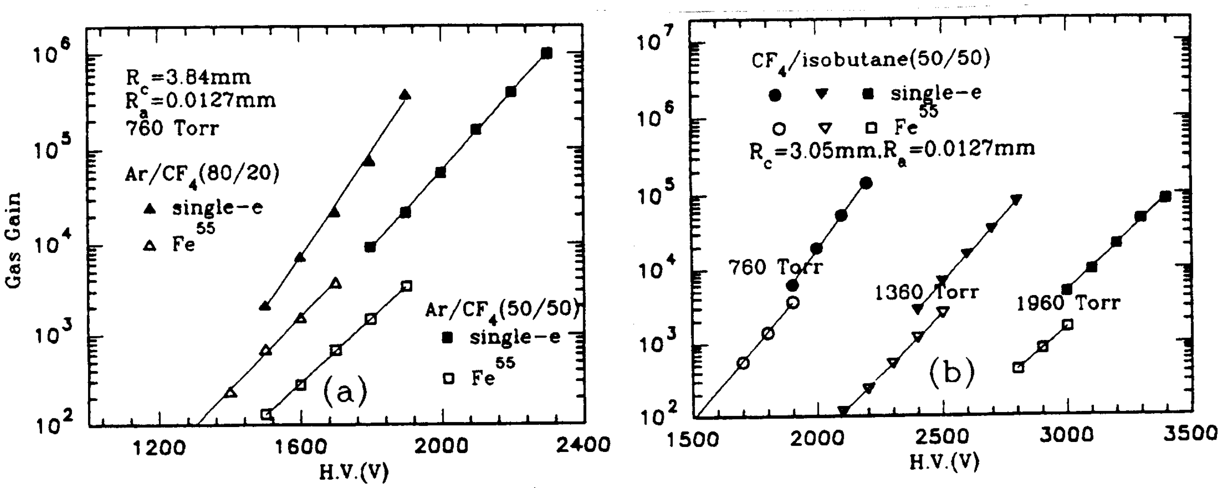

Figure 5: Demonstration of saturated mode at gain of $< 10^4$ for gases with CF_4 [4].

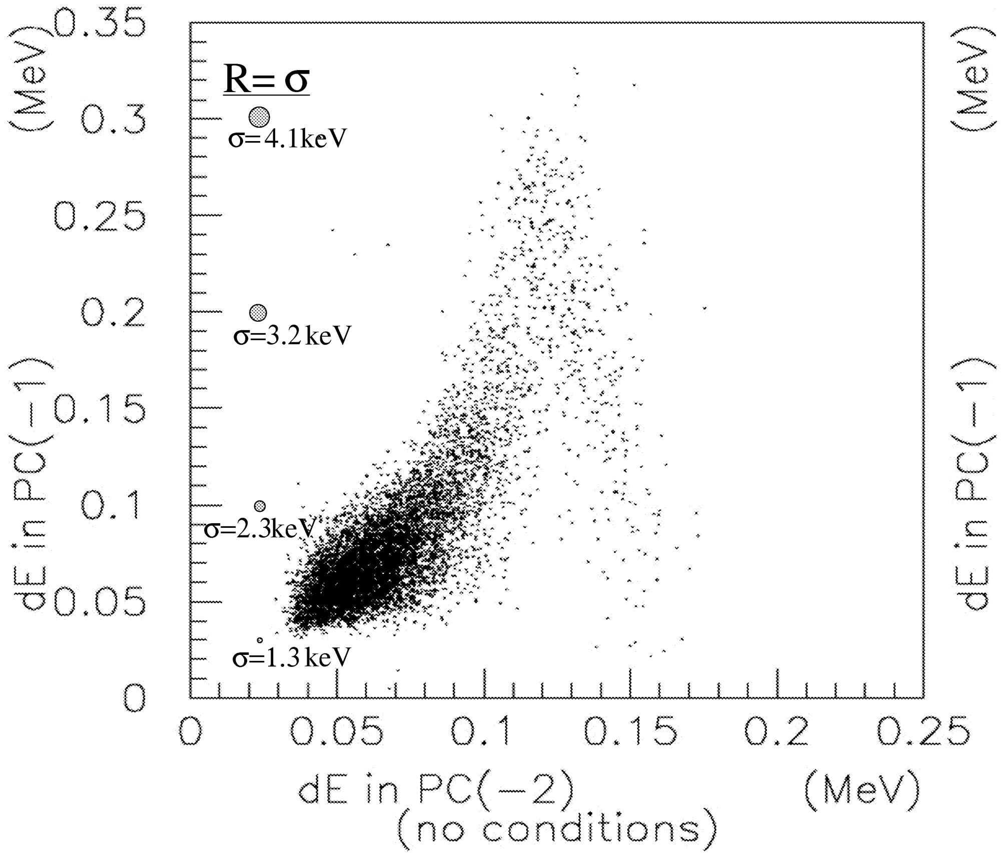

Figure 6: Scatter-plot of a deposit μ^+ energy in PC5 (PC(-2) in the Fig.) and PC6 (PC(-1)) from [5]. The GEANT calculation has been done for all surface muons. Muons stopped in target correspond to deposit energy of 35-120 keV in PC(-2) and of 35-270 keV in PC(-1). The slop from dE=120 keV to dE=150 keV in PC(-2) corresponds to muons stopped in PC(-1). Energy resolution values from Table 1 are presented as circles with radius equals to σ at dE along corresponding to an vertical axis value.

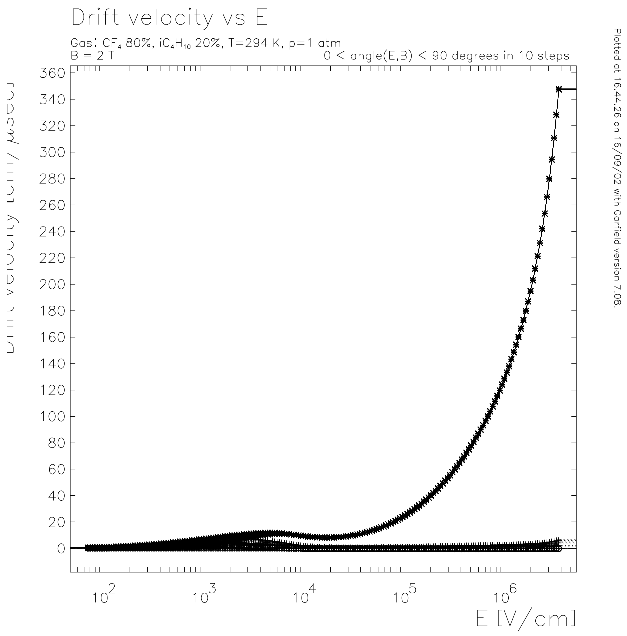

Figure 7: Drift velocity in $CF_4/ISO(80:20)$ gas at $p = 760 Torr$ and $B = 2T$.

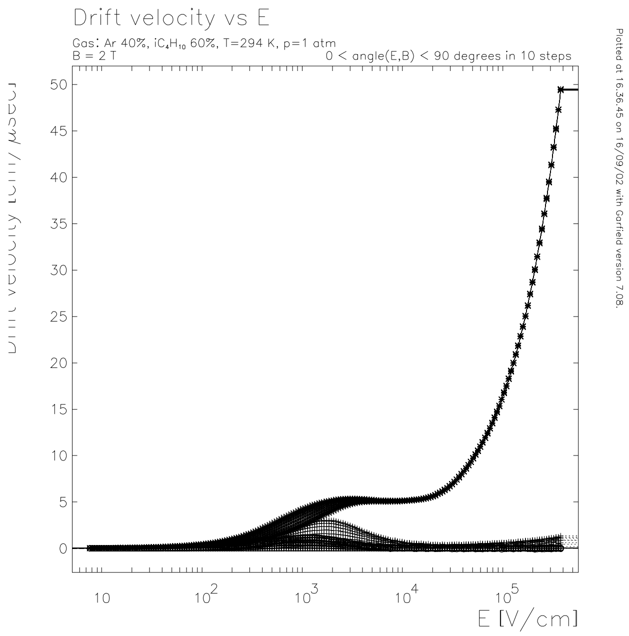

Figure 8: Drift velocity in $Ar/ISO(40:60)$ gas at $p = 760 Torr$ and $B = 2T$.

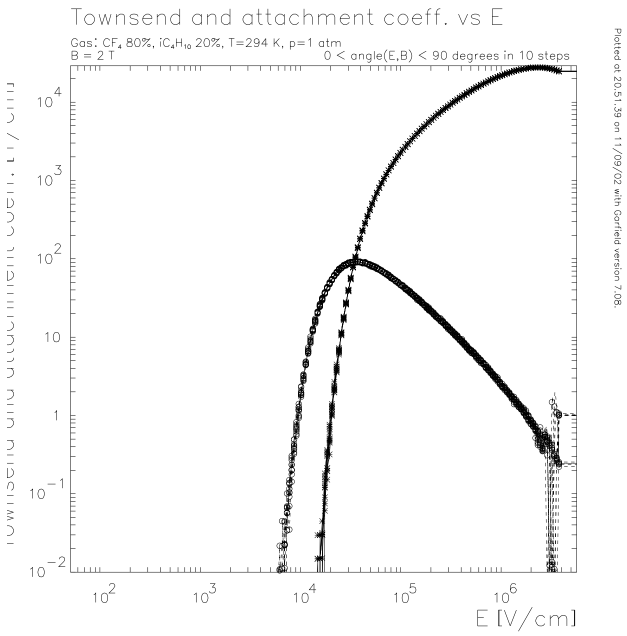

Figure 9: Townsend and attachment coefficients in $CF_4/ISO(80:20)$ gas at $p = 760 Torr$ and $B = 2T$.

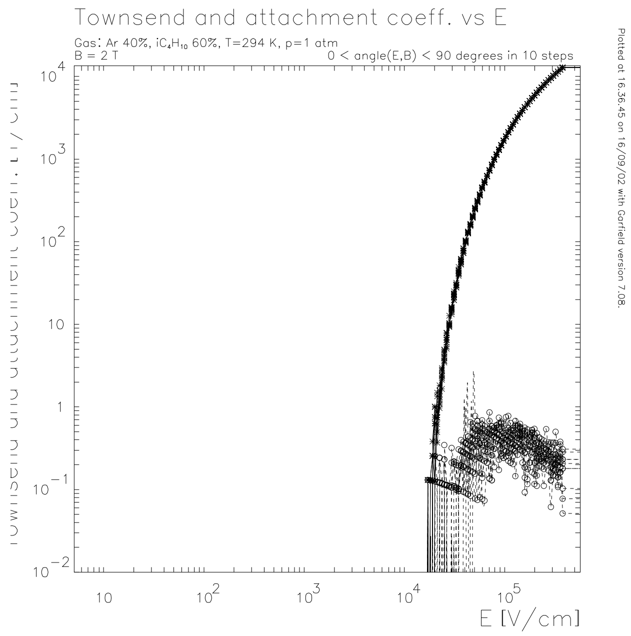

Figure 10: Townsend and attachment coefficients in $Ar/ISO(40:60)$ gas at $p = 760 Torr$ and $B = 2T$.

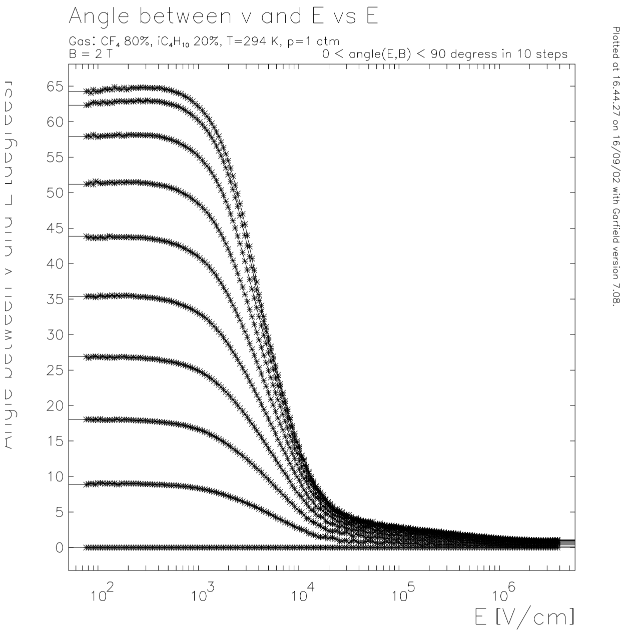

Figure 11: Lorentz drift angle in $CF_4/ISO(80:20)$ gas at $p = 760 Torr$ and $B = 2T$.

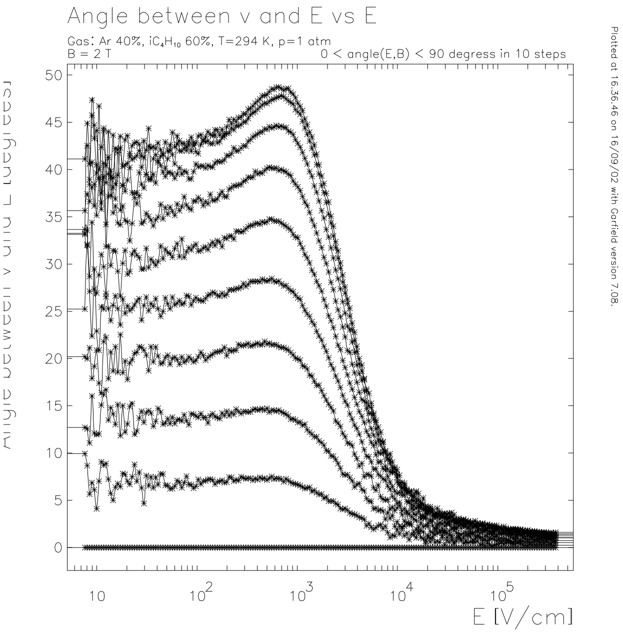

Figure 12: Lorentz drift angle in $Ar/ISO(40:60)$ gas at $p = 760 Torr$ and $B = 2T$.

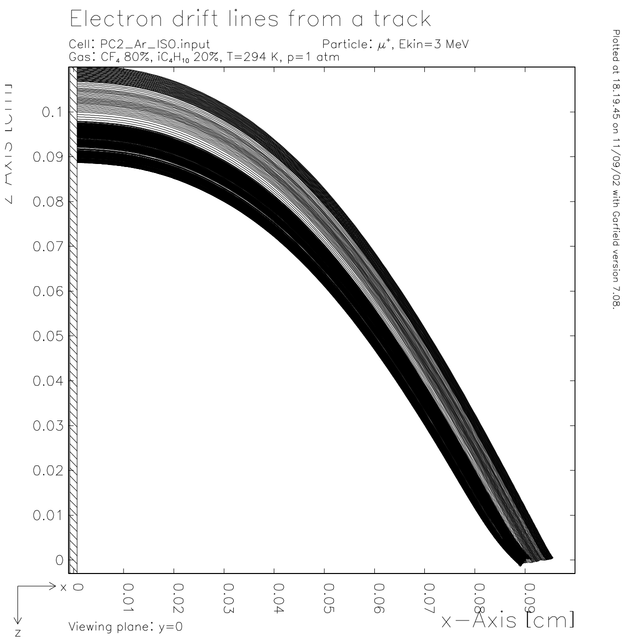

Figure 13: View of muon track and drift electron lines in $CF_4/ISO(80:20)$ gas at $p = 760 Torr$ and $B = 2T$ in Y=0 plane. Sense wire placed at X=0. The track goes originally along Y-axis at X=0.9 mm and Z=0. μ^+ track with $E_{\mu^+} = 3MeV$ in PC at HV=1000 V.

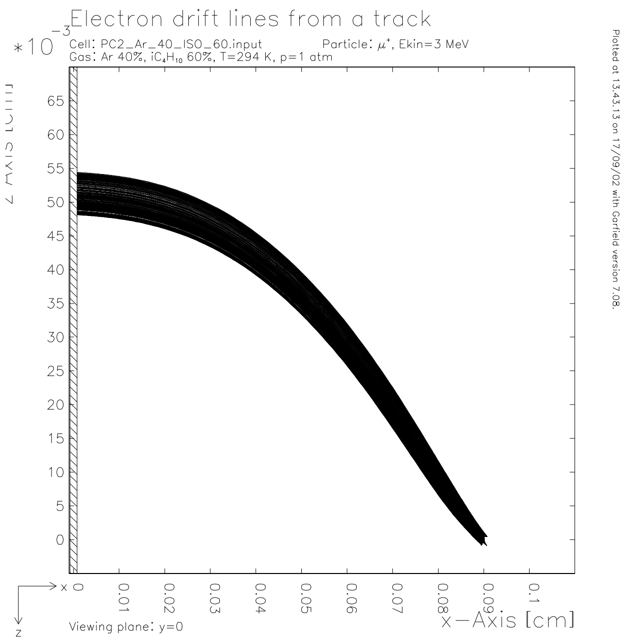

Figure 14: View of muon track and drift electron lines in $Ar/ISO(40:60)$ gas at $p = 760 Torr$ and $B = 2T$ in Y=0 plane. Sense wire placed at X=0. The track goes originally along Y-axis at X=0.9 mm and Z=0. μ^+ track with $E_{\mu^+} = 3MeV$ in PC at HV=1000 V.

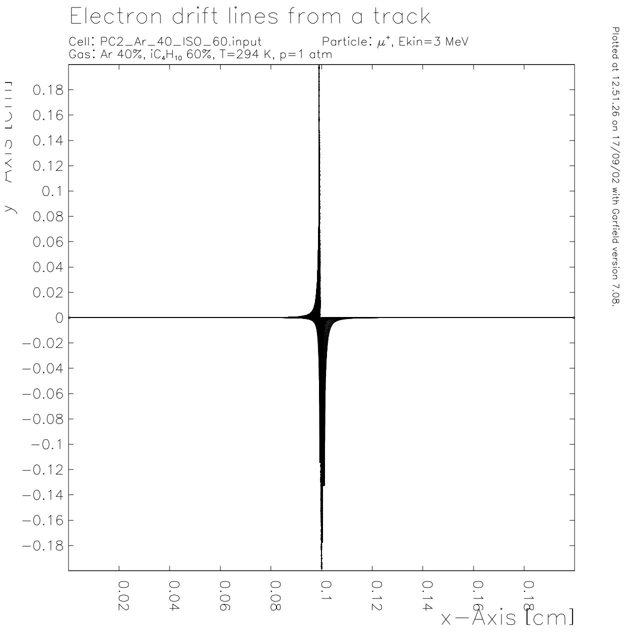

Figure 15: View of muon track and drift lines in $Ar/ISO(40:60)$ gas at $p = 760Torr$ and $B = 2T$ in Z=0 plane. Sense wires placed at X=0 and X=2 mm. The track goes originally along Y-axis at X=1.0 mm and Z=0 exactly along boundary between nearest wires. μ^+ track with $E_{\mu^+} = 3MeV$ in PC at HV=1000 V.

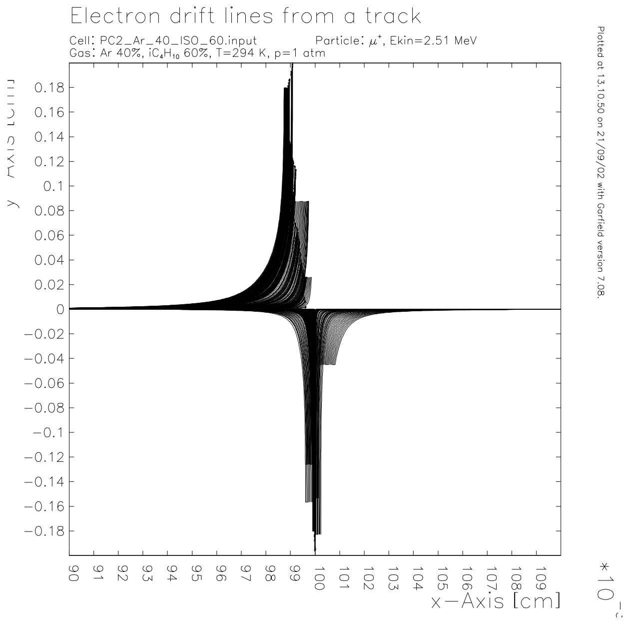

Figure 16: View of the track from Fig.15 inside area $0.9mm < X < 1.1mm$.

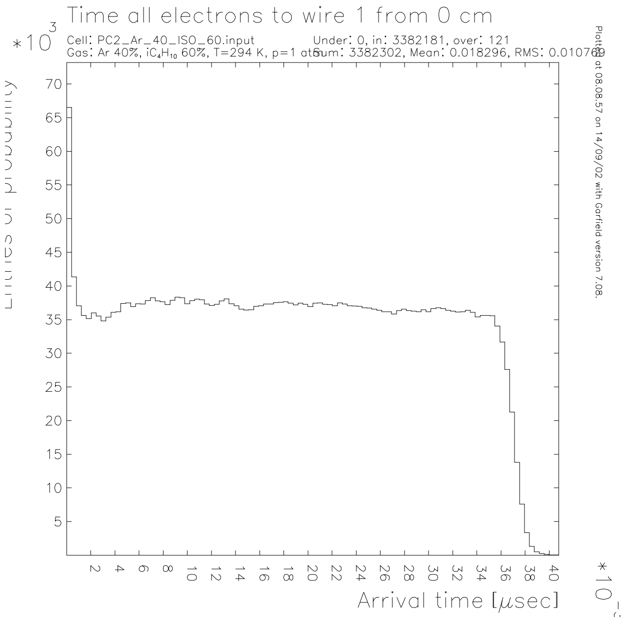

Figure 17: Arrival time of ALL electrons from a μ^+ track going along Y-axis at distance of X=0 from sense wire. $E_{\mu^+} = 1.0MeV$, $Ar/ISO(40:60)$ gas, HV=1000 V. The distribution imitates a signal shape from wire at ideal conditions.

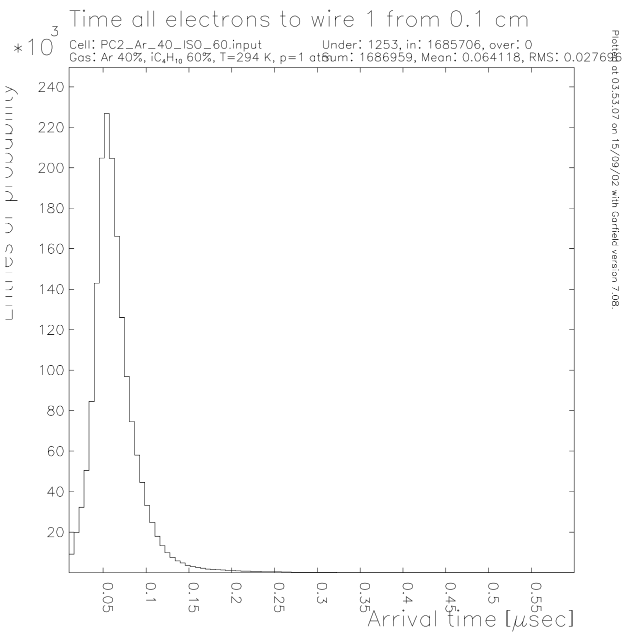

Figure 18: Arrival time of ALL elect-ons from a μ^+ track going along Y-axis at distance of X=1 mm from sense wire. $E_{\mu^+} = 1.0MeV$, $Ar/ISO(40:60)$ gas, HV=1000 V. The distribution imitates a signal shape from wire at ideal conditions.

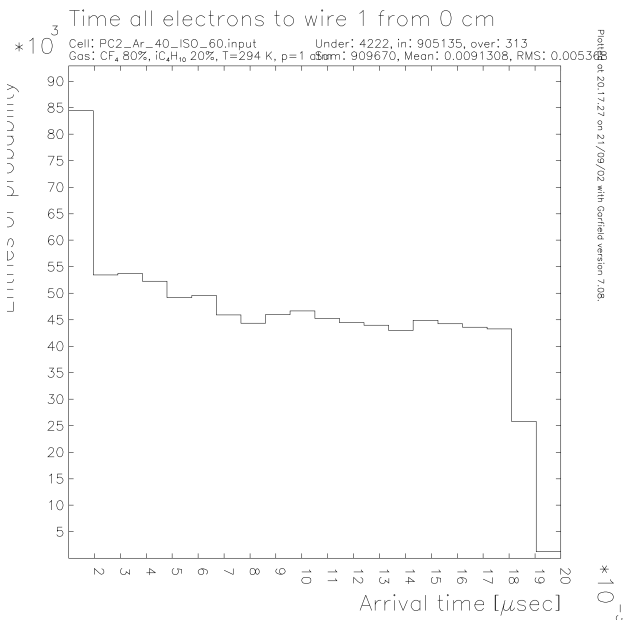

Figure 19: Arrival time of ALL elect-ons from a μ^+ track going along Y-axis at distance of X=0 from sense wire. $E_{\mu^+} = 1.0MeV$, $CF_4/ISO(80:20)$ gas, HV=1000 V. The distribution imitates a signal shape from wire at ideal conditions.

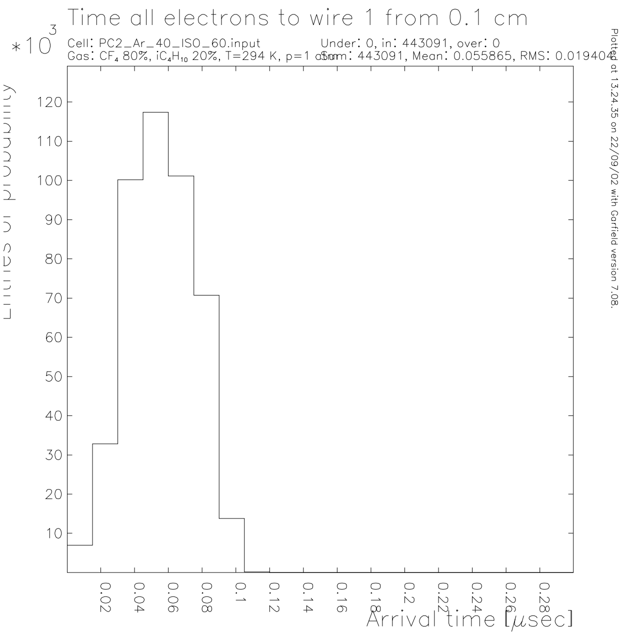

Figure 20: Arrival time of ALL elect-ons from a μ^+ track going along Y-axis at distance of X=1 mm from sense wire. $E_{\mu^+} = 1.0MeV$, $CF_4/ISO(80:20)$ gas, HV=1000 V. The distribution imitates a signal shape from wire at ideal conditions.

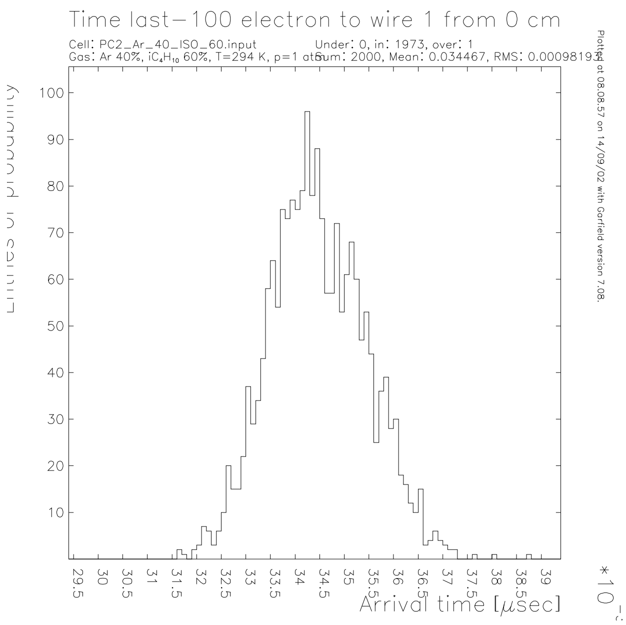

Figure 21: Arrival time of LAST-100 electron from a μ^+ track going along Y-axis at distance of X=0 from sense wire. $E_{\mu^+} = 1.0MeV$, $Ar/ISO(40:60)$ gas, HV=1000 V.

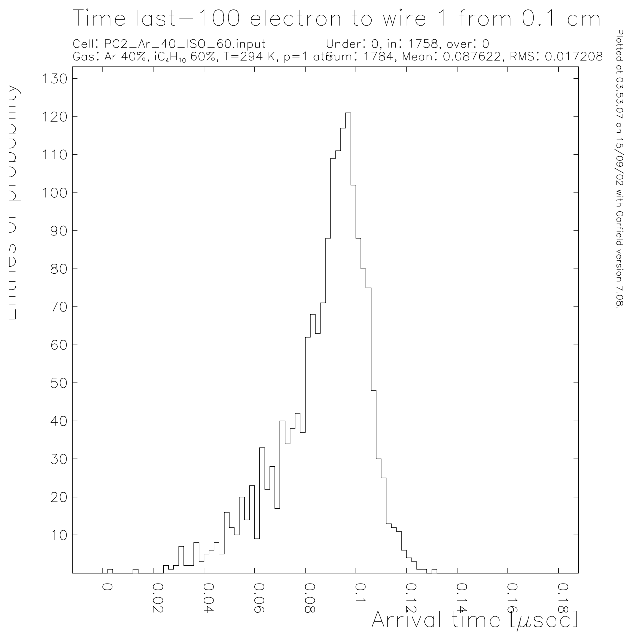

Figure 22: Arrival time of LAST-100 electron from a μ^+ track going along Y-axis at distance of X=1 mm from sense wire. $E_{\mu^+} = 1.0MeV$, $Ar/ISO(40:60)$ gas, HV=1000 V.

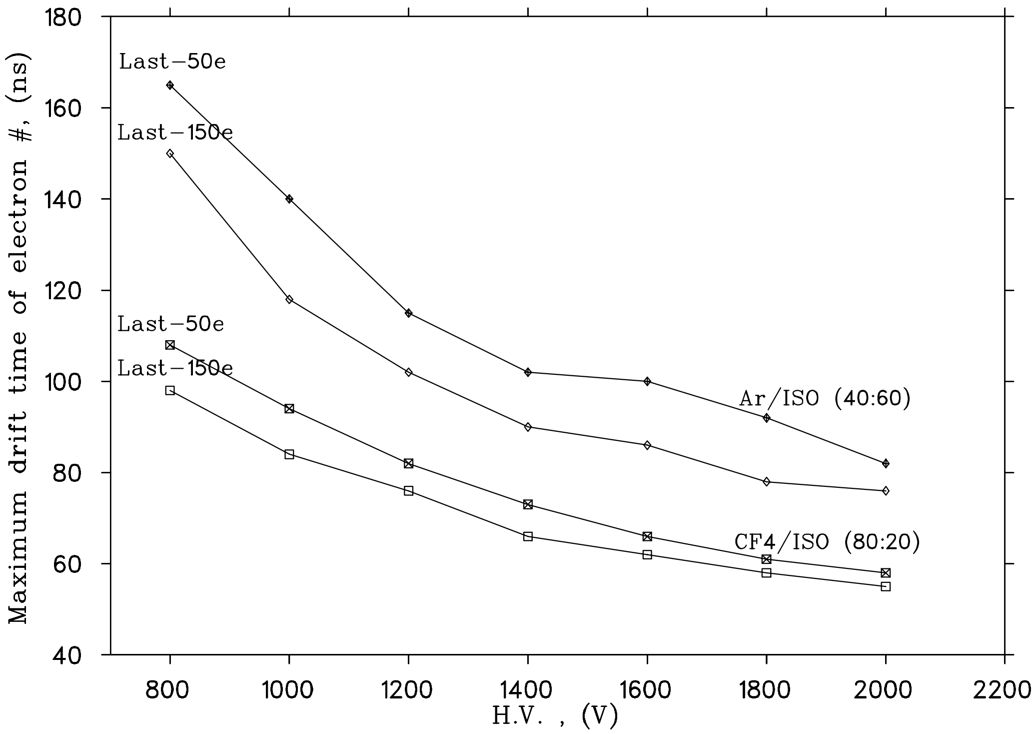

Figure 23: Dependence of maximum drift time for LAST-150 and LAST-50 electron in $CF_4/ISO(80:20)$ and $Ar/ISO(40:60)$ gases vs HV. Muon track with $E_{\mu^+} = 1.0 MeV$ at X=1 mm goes along boundary between nearest sense wires.

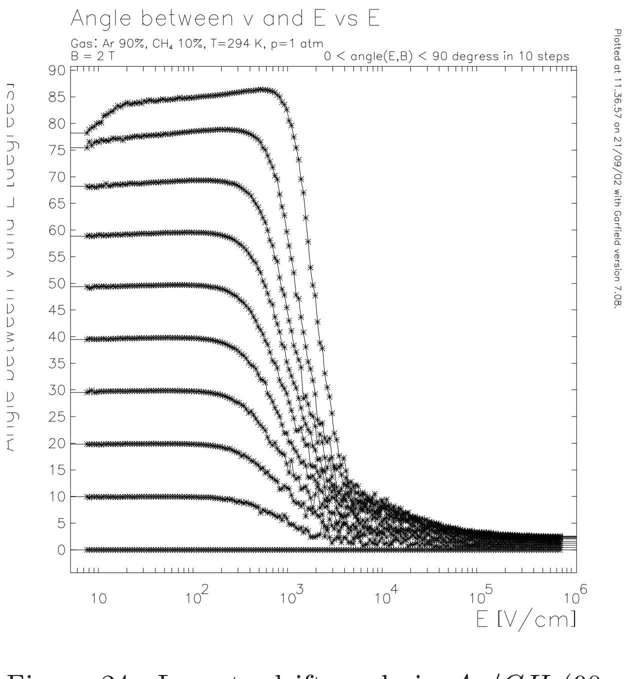

Figure 24: Lorentz drift angle in $Ar/CH_4(90:10)$ gas.

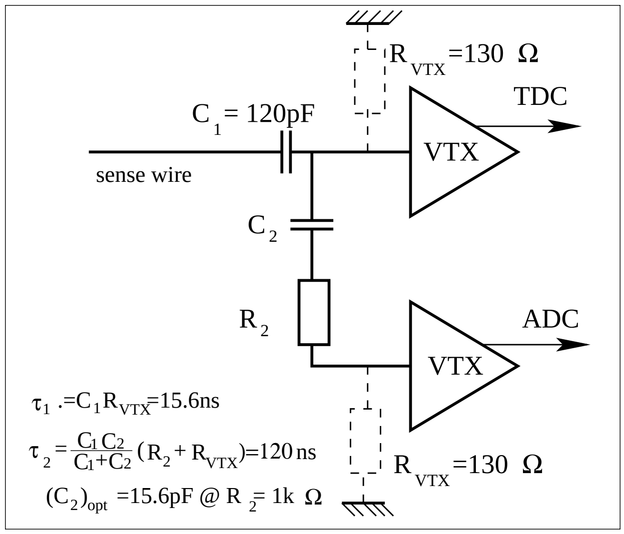

Figure 25: Sketch of a sense wire output in target PCs.

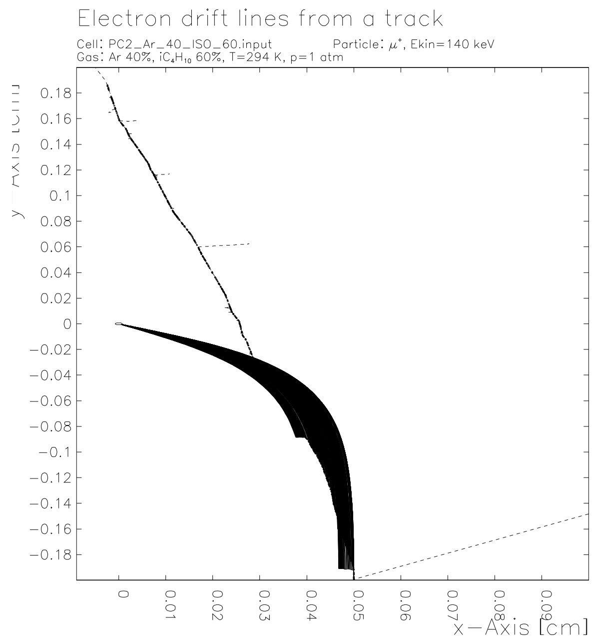

Figure 26: Muon track with $E_\mu = 140keV$ in PC. GARFIELD skipped most part of drift lines because an overflow. Muon has been scattered on $\simeq 0.5mm$ in X-direction and stops in gas. One can see γ left the cell from point with X=0.05cm and Y=-0.19cm.

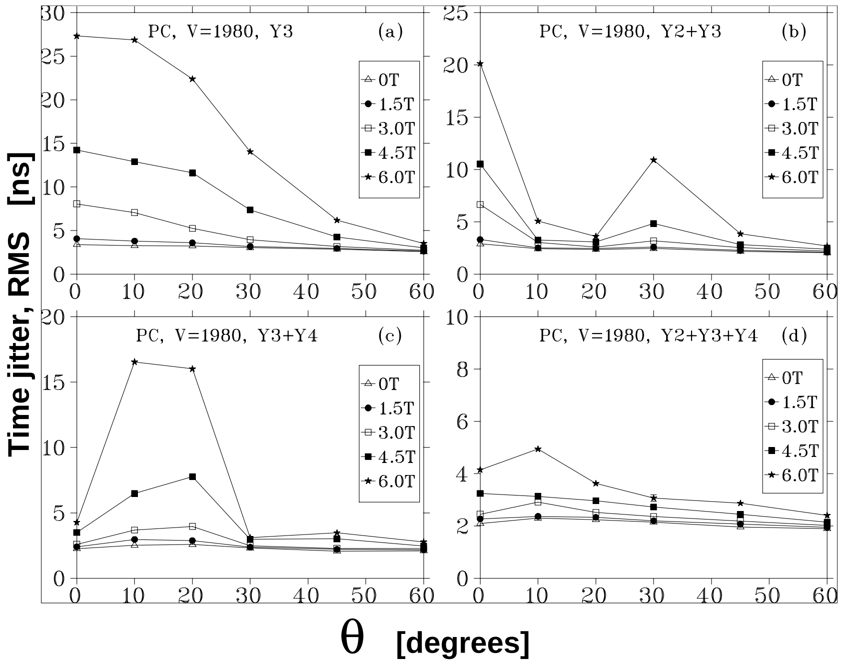

Figure 27: Time resolution as a function of θ and magnetic field B for (a) one plane, (b,c) two planes, (d) three planes. PC with our sizes and $CF_4/ISO(80:20)$ gas have been used. Each Y2, Y3 and Y4 chamber consists of 36 sense wires. Measurements been done in a magnetic field to 6.0 T using HELIOS magnet and positrons with $p = 50MeV/c$ from M15 beam line. Chamber Y4 has been shifted on 1mm relative to Y2 and Y3. The θ is angle between B direction and perpendicular to chamber plane [7].